Supplemental Information

Table S1. Ubiquitin-like protein architecture in Bil and Bub operons

See separate Excel workbook

Table S2. Proteins used in this study

Species	Operon type	Ubl type	Accession	Sequence
Methylobacterium brachiatum DSM19569	Type II Bil	Ubl_3	IMG 2928979547	MHEHEHVEDRVAVQVFDENLNAKDVHLTDPVPTGRQIIKAA GKHPVDDYAVLAWMPDNALRPLHLDETFDLRQHGVERILVA PSDTLYRFFIDGQDQEWPVRGITGVVLKTLAGVDPAAFEVFL VIPGDDDIRVEDHELFDLARKGVEHFQTVKRKAPAEHGIALK VVVNGTETELKVHAGTPLRQVRTEALQKSGNVGRPEDEWQ LKDEHGNPYDLNQTVAGVGLHDGDLVWLSLNAGVAGV
Citrobacter sp. RHBSTW-00271	Type I Bub	Ubl_3	IMG 2938140956 (Ubl-E2 fusion; E2 fragment not included)	MQDIQSQHHHRRFIEVADETLSFRQVVMEDSTPNGSQISAA SGFKPDQMPVVLMLLPNGSLEDIRPDEVVDLSSEVRRFIVVE SDRTYFFTIDGARLEWPCRFITGYSIRQLGDIGDNKKLLLERE DEADLEVQNDQIIDLDGDGIERFISRKATWKLNIQGKEFTFDT PTVVIRDAVIRAGLNPNQAWHIFLKVEGQPKVEKNIDDVIDLR TPGIEKLRLTPKDVNNGEEPRATRRDFSLRPEDEHYLDEMG YCWETRLVGNARWLIIHDYELPDGYNHHQVNLALLITSGYPV NMLDMFYVYPPLVRVNGVNIPATEATVAIDSVAYQRWSRHR SWNPEIDSVISQLAMADGCLQKEVGQ
E. coli ZDHYS365	Type II Bub	Ubl_3	NCBI WP_053069300.1	MKNKFIKINDKIVEIDDLTPTGAQILLVAGVKDIVEYVLFQKLK NGLLEEIRPEEKTTLDKEGVETFLMFNSDRTYRFTLNGKMFD WGAPSLTGATVKSLAECDFDSNDVWLEMKNEKDKLITDHEH IDLTQPNVERLYTQETSINIIVNAKMRVVNRRVISYWDVVHLA YEHAENKETSIYSVDYAKGPISNPEGSMVDGQYVQLTDGMI FYVTQTDKS
Bradyrhizobium sp. Ghvi	Type I Bub	Coiled-coil-Ubl_1	IMG 2653856993	MTEHDEAGAPTKREKELKAFRERQMRELREFEQRQKQELE EFERQELEELKEFEERQHPYEIKIDRTEFKVTEHFLTGAQLR ALPNPPIGPERDLFEVVPGGSDEKIADTQKVKMRDGLRFFTA PAQINPGLL
Bradyrhizobium nanningense CCBAU 53390	Type II Bil	Coiled-coil-Ubl_1	IMG 2874628352	MSAVHDNAGFGPERLANMSESGNKSAEQFDREAEFLKKEIE GVNEVIRSEEKIKHDLEKREHELEEEARRREKHDHDHDHG HLVRITMVVNGQPVVIEAEEKEKLTEIRQKALQETQNLAQPA ENWEIKDEAGAVLDPEKRVGEYHFGKEVTLFLSLKAGVAG
Pseudanabaena sp. PCC 7367	Type I Bub	Ubl_2	IMG 2504678157 (Ubl-E2 fusion; E2 fragment not included)	MISTKKIQVQIDEKTYFVEDPVITGLQLLEKAEKRPSDEYLIFY LLPGGQLEEIRLDETVDLRQMGIERFITWRSDRSFRLVIDGR RFEWGIPIITGIQLKKLAGVDPKAYGIWLEVRGGEDRPIENAE EVNLDAEGVERFFTGKKTTTEGQNAILLPSQDREYLKSRSLD FEEIVDGSKCGVVFPGFPLPTQFDANQTDLLLILPSGYPDAP PDMFFLDPWIKLRQGNCFPKAANQPYAFDGRSWQRWSRH NREWRPGVDGIWTMLKRVEHALEVAA
Bradyrhizobium sp. WSM1417	Type II Bub	Ubl_2	IMG 2507506256	MTDAKHEVRIHIDQKPYHSPNPTTGADLYELGHVAEGKVLY KEVEGDHEDKLVRIDSPSIHLTEDEHFHSGDAPEKHYTIIVNT DPVVVDHDVLTFEELVKIAYPVPPTGLDPEFTVSFEHAKSVP HHGDLPPNGKVTVKKHGTIFDVDHTNRS
Photobacterium chitinilyticum BEI 247	Type II Bub	DUF1508-Ubl_1	IMG 2885240117	MKGKFEIFQSSKNNEYYFRLKAAGNWEIILDSEGYTTKSSCL NGIESVKENAQLEERFERLVAKNGEHYFNLKAGNGQVIGTS EMYTRRQGMENGIHSVMKNAPDADIKDLTIDEPEHDKEFNII VNGRPKTVTSKILTFEDIVKLAFSTIADGNSTIYTMTYKKNGG NKPEGTLVTGDQIKIKSGVIFNVTATDKS
Marinifilum flexuosum isolate 1468	Type II Bub	DUF1508-Ubl_1	NCBI WP_282016492.1	MNSYFTIKVGKDDQYYFNLKAGNHEIILQSEGYENKSGTLNG IESVRLNSQIRSNFEIRYSKRNEPYFVL KAPNGKIIGCSEMYSSVHAMENGIHSVMKNGNTPKIHDLTDD DHEGKERQIVVNGRVKTWNQKYIEFKEL VELAFGSYNDNPNTCYTITYTRGCSNKPQGSIVKGEEVKVK PKMIFNVTATDKS

Table S3. Crystallographic data collection and refinement

	E. coli Ubl_3	*M. brachiatum* Ubl_3
Data collection		
Data collection date	August 30, 2022	March 2, 2023
Beamline	ALS 5.0.1	APS 24ID-C
Wavelength (Å)	0.97741	0.97911
Space group	$P3_221$	$P3_121$
Cell dimensions		
a, *b*, *c* (Å)	117.54, 117.54, 104.44	136.02, 136.02, 105.51
α, β, γ (°)	90, 90, 120	90, 90, 120
Resolution (Å)*	46.5-1.87 (1.91-1.87)	117.8-3.04 (3.22-3.04)
R_{merge}	0.093 (2.232)	0.204 (3.416)
$I / \sigma I$	16.1 (0.8)	14.0 (0.9)
Completeness (%)	100 (100)	99.9 (99.9)
Redundancy	9.5 (6.1)	10.0 (10.4)
Refinement		
Resolution (Å)	46.46-1.87	117.80-3.04
No. reflections	69064	22023
R_{work} (%)	18.16 (33.16)	23.86 (39.41)
R_{free} (%)	21.27 (35.77)	27.62 (39.99)
No. atoms		
Protein (non-H)	3526	4779
Ligand/ion (non-H)	28	31 (Ca^{2+}, PO_4^-)
Water	537	53
Hydrogen	3511	0
B-factors		
Protein	41.7	114.5
Ligand/ion	53.7	139.9
Water	45.5	98.5
R.m.s. deviations		
Bond lengths (Å)	0.017	0.003
Bond angles (°)	1.399	0.57
Validation		
MolProbity score	1.07	1.11
Clashscore	2.12	3.22
Poor rotamers (%)	1.30	0.40
Ramachandran plot		
Favored (%)	98.77	99.49
Allowed (%)	1.23	0.51
Disallowed (%)	0	0
PDB ID	9CD2	8U38
SBGrid Data Bank ID	1115	1043

*Values in parentheses are for highest-resolution shell.

Table S4. CryoEM data collection and refinement

	Citrobacter Ubl$_3$ (global)	*Citrobacter* Ubl$_3$ (local)	*M. brachiatum* Ubl$_3$
Data collection and processing			
Magnification	130,000		105,000
Voltage (kV)	300		300
Electron exposure (e–/Å^2)	45		50
Defocus range (μm)	-2.0 to -1.2		-2.0 to -1.2
Pixel size (Å)	0.935		0.822
Symmetry imposed	Helical and D1		Helical and D1
Initial particle images	1,634,973		495,217
Final particle images	1,258,222 (D1 symmetry expanded)	148,697	151,090
Map resolution (Å; 0.143 FSC)	2.43	2.73	3.08
Refinement	*Global (4 protomers)*	*Local (1 protomer)*	*Global (4 protomers)*
Model resolution (Å; 0.143 FSC)	2.4	2.7	3.1
Model composition			
Non-hydrogen atoms	4698	1704	4650
Protein residues	584	212	584
Ligands (Ca^{2+})	14	5	10
B factors (Å^2)			
Protein	85.1	124.9	125.7
Ligand	108.1	110.0	90.2
R.m.s. deviations			
Bond lengths (Å)	0.002	0.004	0.002
Bond angles (°)	0.384	0.431	0.471
Validation			
MolProbity score	1.15	1.32	1.72
Clashscore	3.56	5.59	6.09
Poor rotamers (%)	0.76	1.05	3.23
Ramachandran plot			
Favored (%)	98.61	99.05	99.31
Allowed (%)	1.39	0.95	0.69
Disallowed (%)	0	0	0
PDB ID	9D59	9D5A	9D5B
EMDB ID	EMD-46576	EMD-46577	EMD-46578

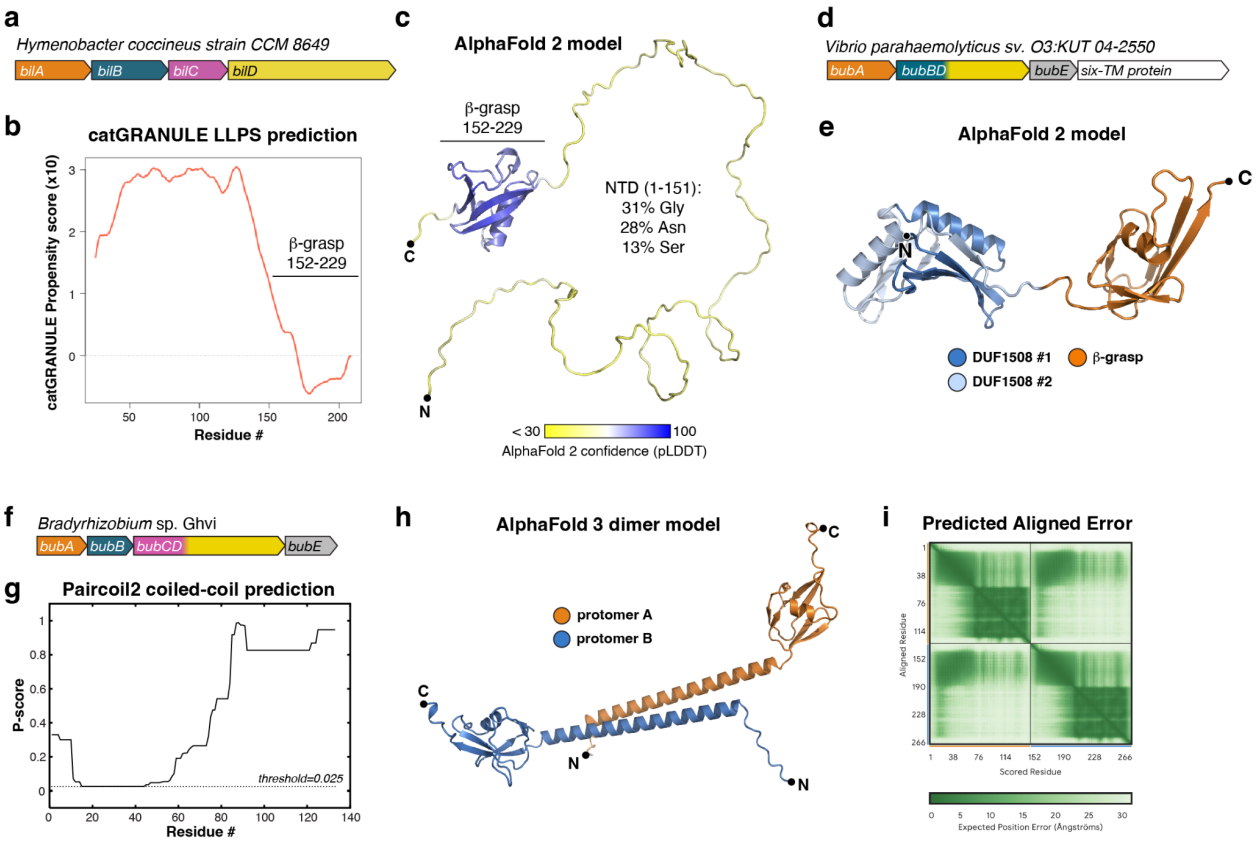

Figure S1. Bacterial ubiquitin-like proteins show diverse architectures. (a) Operon schematic of a *Hymenobacter* Type II Bil operon whose BilA protein (IMG Gene ID 2625034186) N-terminal domain is predicted to be disordered. **(b)** catGRANULE analysis of *Hymenobacter* BilA showing that its disordered N-terminal domain has a high propensity to undergo liquid-liquid phase separation. **(c)** AlphaFold 2 model of *Hymenobacter* BilA colored by confidence (pLDDT). The sequence composition of the disordered N-terminal domain is noted. **(d)** Operon schematic of a *Vibrio* Type II Bub operon whose BubA protein (IMG ID 2704903835) N-terminal domain is predicted to encode tandem DUF1508 domains. **(e)** AlphaFold2 model of *Vibrio* BubA, with DUF1508 domains colored dark/light blue and β-grasp domain dark orange. See **Figure S2c-d** for SEC-MALS analysis of two DUF1508-Ubl1 proteins. **(f)** Operon schematic of a *Bradyrhizobium* Type I Bub operon whose BubA protein (IMG ID 2653856993) N-terminal domain is predicted to form a coiled-coil. **(g)** PairCoil2 analysis of *Bradyrhizobium* BubA, showing a predicted coiled-coil domain at the N-terminus. **(h)** AlphaFold 3 model of a *Bradyrhizobium* BubA dimer, with one protomer colored dark orange and the second protomer colored dark blue. See **Figure S2e** for SEC-MALS analysis of this protein, and **Figure S2f** for SEC-MALS analysis of a second predicted CC-Ubl$_1$ protein. **(i)** AlphaFold 3 predicted aligned error plot for the *Bradyrhizobium* BubA dimer shown in panel (H), showing high confidence for interactions between dimer-related coiled-coil N-terminal domains.

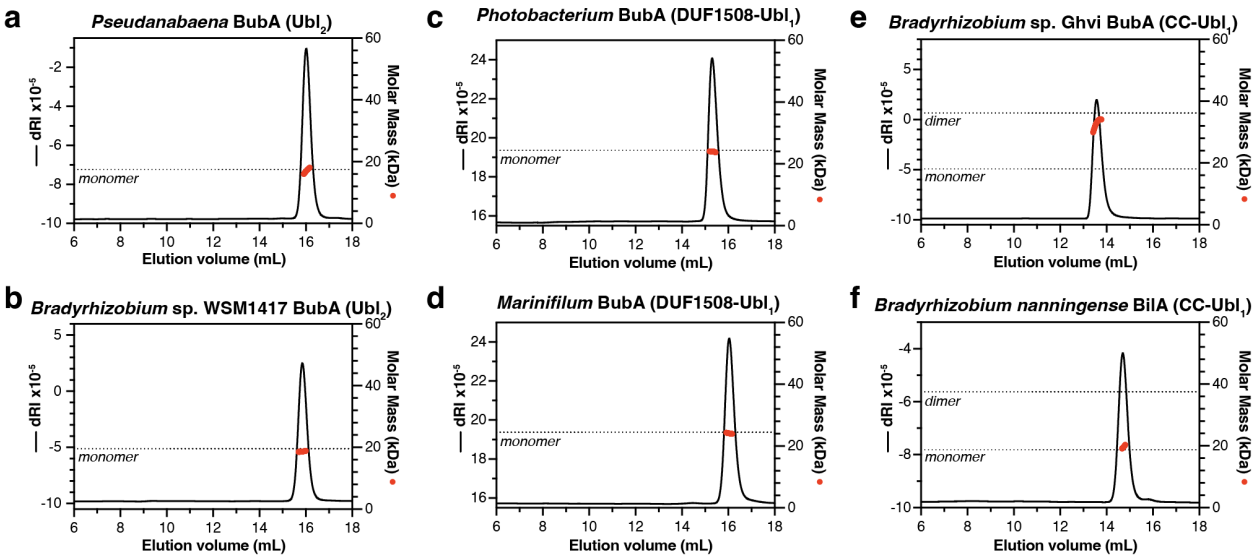

Figure S2. SEC-MALS analysis of bacterial Ubl proteins. (a) SEC-MALS analysis of *Pseudanabaena* sp. PCC 7367 BubA (see **Table S2** for accession numbers and protein sequences), which possesses two β-grasp domains. Differential refractive index (dRI; measuring protein concentration) is shown as a black line, and measured molar mass is shown as red circles. The predicted molar mass of a monomer is shown as a dotted line. **(b)** SEC-MALS analysis of *Bradyrhizobium* sp. WSM1417 BubA, which possesses two β-grasp domains. The predicted molar mass of a monomer is shown as a dotted line. **(c)** SEC-MALS analysis of *Photobacterium chitinilyticum* BEI 247 BubA, which possesses a single β-grasp domain and a predicted DUF1508 N-terminal domain. The predicted molar mass of a monomer is shown as a dotted line. **(d)** SEC-MALS analysis of *Marinifilum flexuosum* isolate 1468 BubA, which possesses a single β-grasp domain and a predicted DUF1508 N-terminal domain. The predicted molar mass of a monomer is shown as a dotted line. **(e)** SEC-MALS analysis of *Bradyrhizobium* sp. Ghvi BubA, which possesses a single β-grasp domain and a predicted coiled-coil N-terminal region. The predicted molar mass of a monomer and a dimer are shown as dotted lines. **(f)** SEC-MALS analysis of *Bradyrhizobium nanningense* CCBAU 53390 BilA, which possesses a single β-grasp domain and a predicted coiled-coil N-terminal region. The predicted molar mass of a monomer and a dimer are shown as dotted lines.

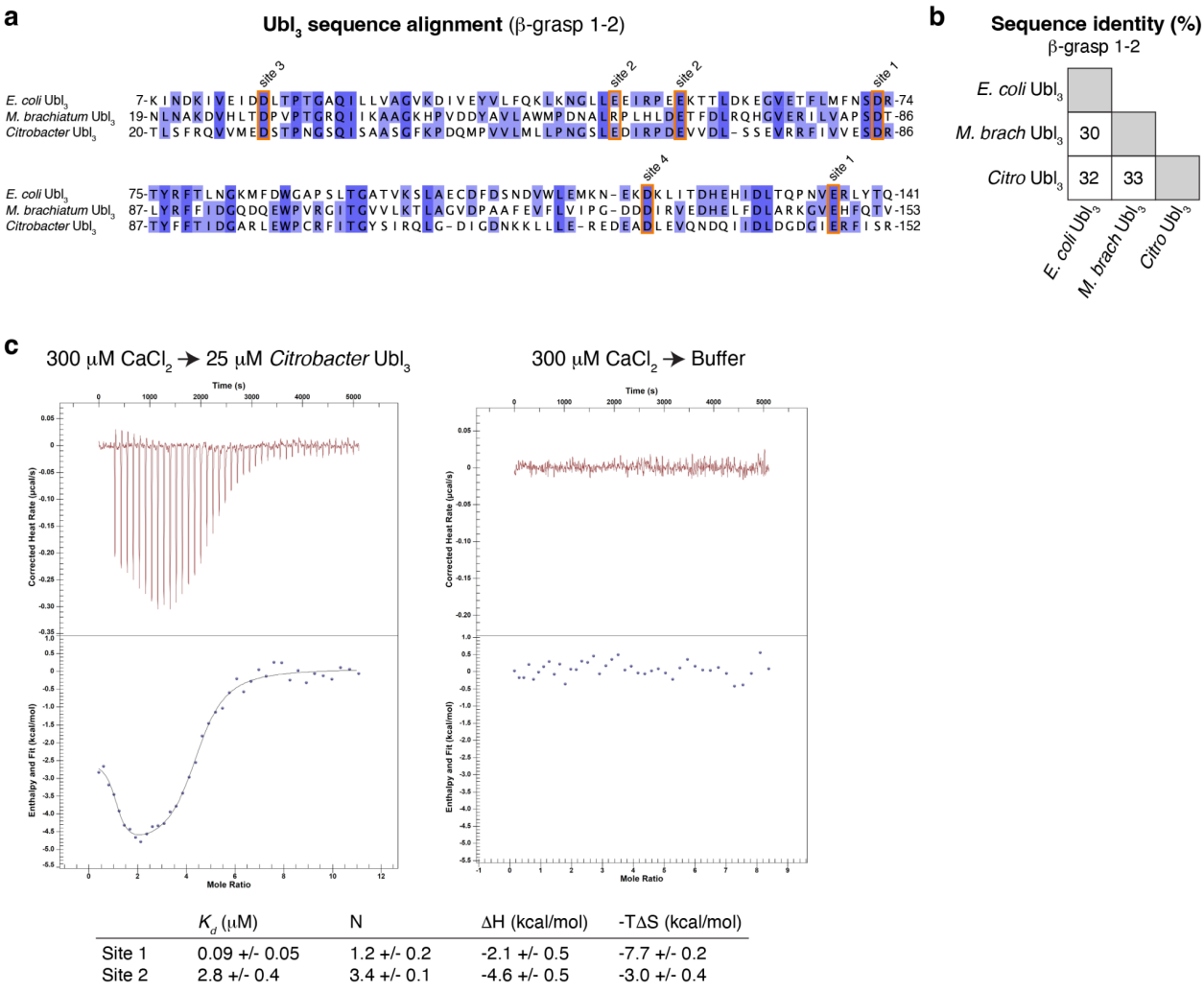

	K_d (μM)	N	ΔH (kcal/mol)	-TΔS (kcal/mol)
Site 1	0.09 +/- 0.05	1.2 +/- 0.2	-2.1 +/- 0.5	-7.7 +/- 0.2
Site 2	2.8 +/- 0.4	3.4 +/- 0.1	-4.6 +/- 0.5	-3.0 +/- 0.4

Figure S3. Sequence alignments and Ca^{2+} binding of Ubl_3 proteins. (a) Sequence alignment of β-grasp domains 1 and 2 from the three Ubl_3 proteins under study (see **Table S2**), with residues involved in Ca^{2+} ion coordination outlined in orange. **(b)** Table of protein sequence identities for the three Ubl_3 proteins in panel (a). **(c)** Isothermal titration calorimetry for *Citrobacter* Ubl_3 binding $CaCl_2$. *Left:* Binding data (top) and fit curve (bottom); trace is representative of four independent trials. Right: No-protein control injection series. Bottom: Data from four independent trials was fit using a two-site binding model. N designates molar equivalent of ligand binding.

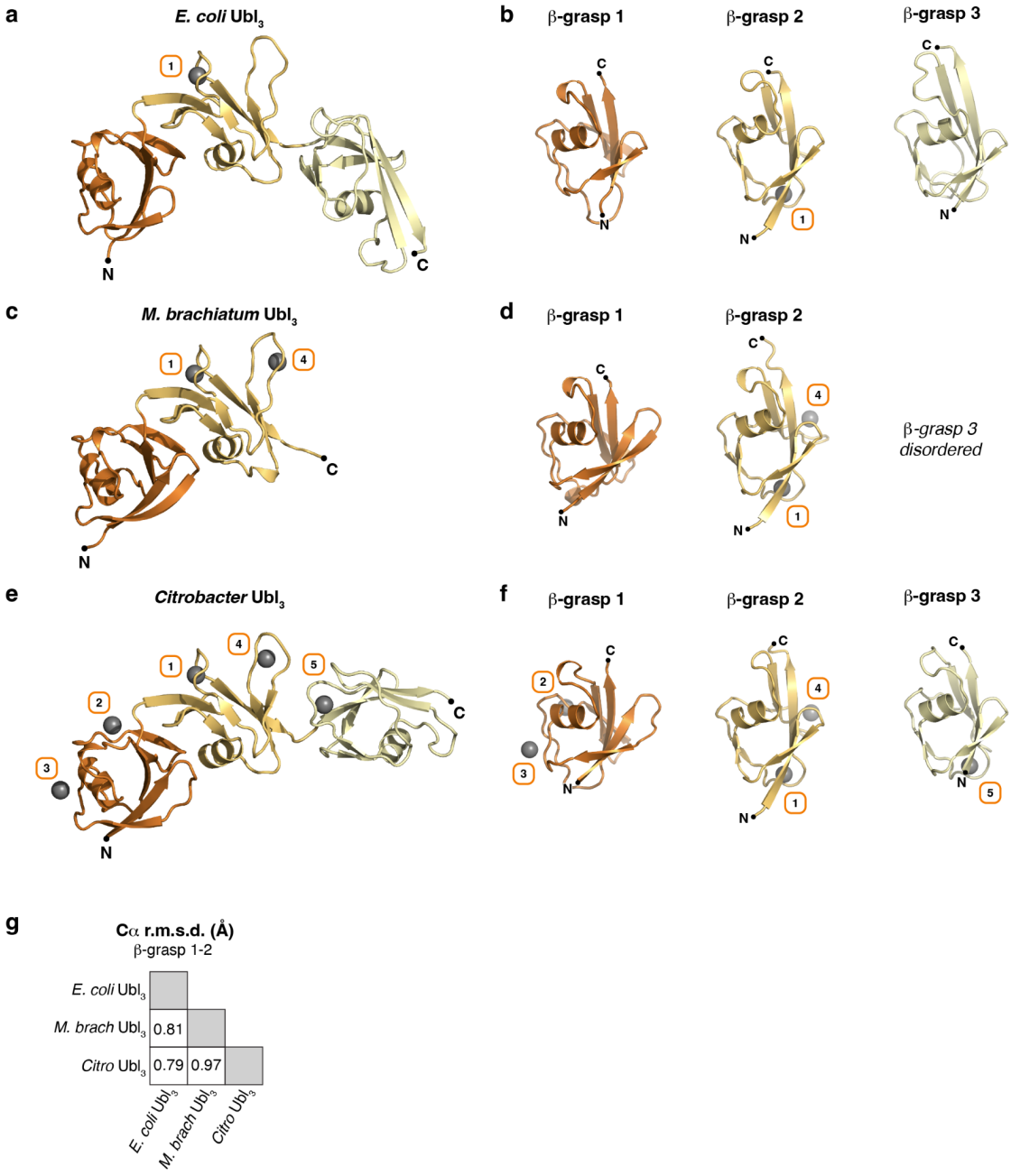

Figure S4. Structures of Ubl$_3$ proteins. (a) Structure of an *E. coli* Ubl$_3$ monomer, with β-grasp domains 1-3 colored dark orange, light orange, and light yellow, respectively. Bound Ca^{2+} ions are shown as gray spheres and labeled with the site number (according to *Citrobacter* Ubl$_3$ Ca^{2+} site numbering). **(b)** Structures of *E. coli* Ubl$_3$ β-grasp domains 1-3. **(c)** Structure of an *M. brachiatum* Ubl$_3$ monomer. β-grasp domain 3 is disordered and not shown. **(d)** Structures of *M. brachiatum* Ubl$_3$ β-grasp domains 1-2. **(e)** Structure of a *Citrobacter* Ubl$_3$ monomer. **(f)** Structures of *Citrobacter* Ubl$_3$ β-grasp domains 1-3. **(g)** Table of structural similarity between three Ubl$_3$ proteins, spanning β-grasp domains 1 and 2. Cα r.m.s.d.: average root mean squared displacement between aligned alpha-carbon atoms. Comparison of *E. coli* and *Citrobacter* Ubl$_3$ β-grasp domain 3 shows higher divergence, with a 3.1 Å overall Cα r.m.s.d. in this domain.

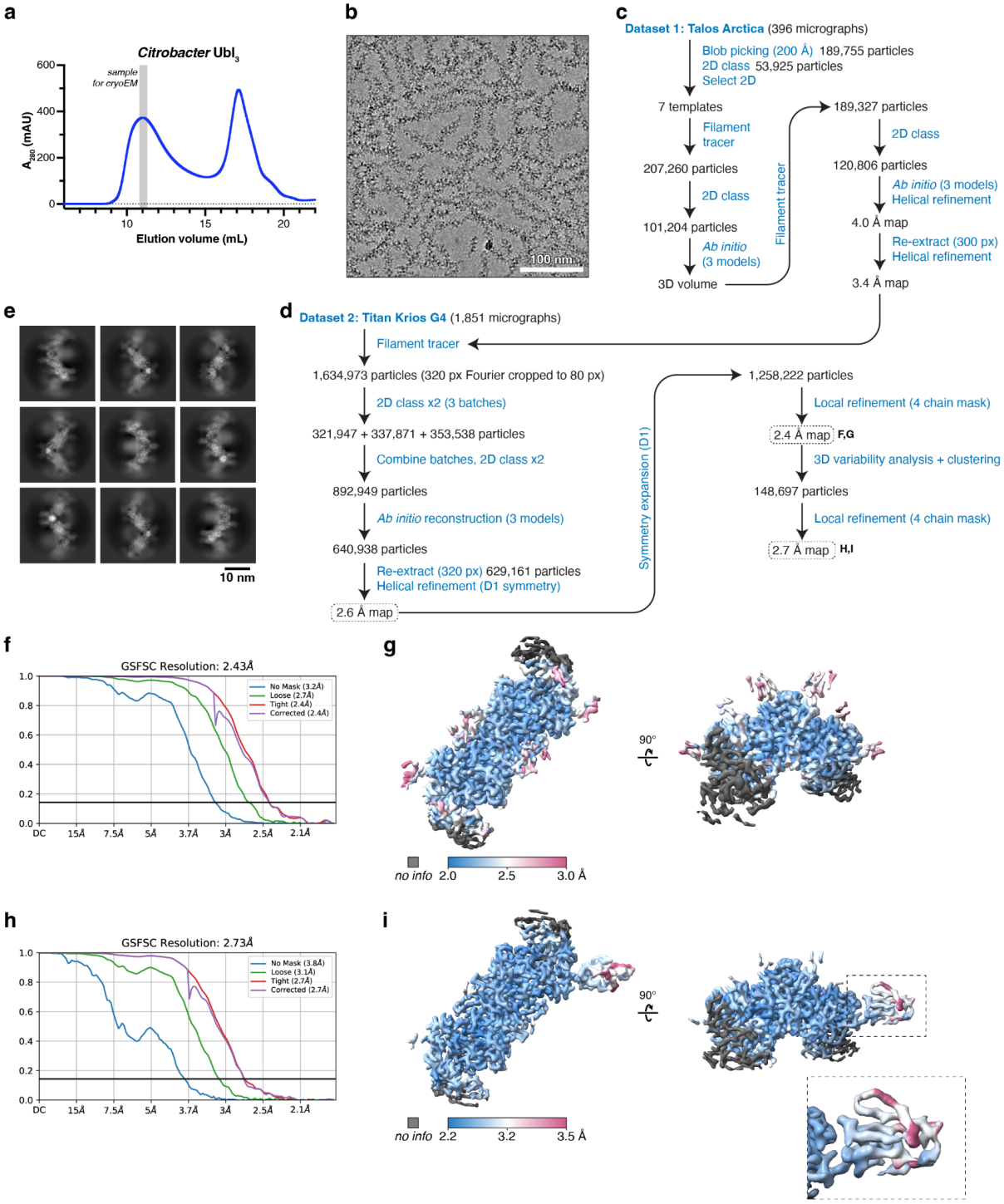

Figure S5. CryoEM structure of a *Citrobacter* Ubl$_3$ filament. (a) Size exclusion chromatography elution profile of purified *Citrobacter* Ubl$_3$, with the fraction used for cryoEM analysis highlighted in gray. **(b)** Raw cryoEM micrograph of *Citrobacter* Ubl$_3$. **(c)** CryoEM structure determination workflow for preliminary dataset. **(d)** CryoEM structure determination workflow for final dataset. **(e)** Selected 2D classes from final dataset. **(f)** Fourier Shell Correlation graph for global refinement (four Ubl$_3$ protomers masked). **(g)** Local resolution of

final globally refined cryoEM map (four Ubl_3 protomers masked). **(h)** Fourier Shell Correlation graph for local refinement with particle subset selected from 3D variability analysis to reveal β-grasp domain 3 in one protomer (four Ubl_3 protomers masked). **(i)** Local resolution of local refinement with particle subset selected from 3D variability analysis to reveal β-grasp domain 3 in one protomer (four Ubl_3 protomers masked).

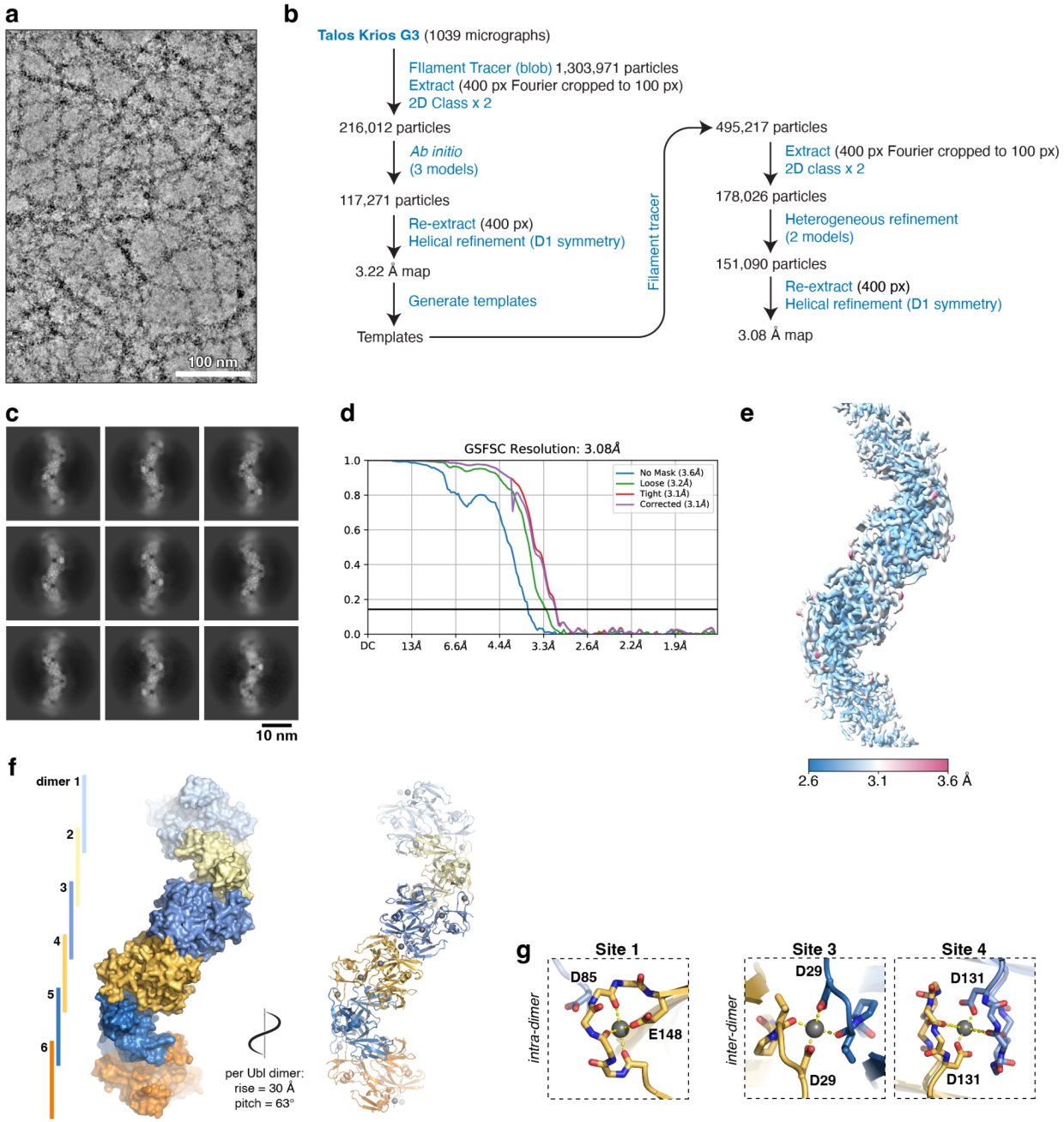

Figure S6. CryoEM structure of an *M. brachiatum* UbI_3 filament. (a) Raw cryoEM micrograph of *M. brachiatum* UbI_3 after incubation with 5 mM $CaCl_2$. **(b)** CryoEM structure determination workflow. **(c)** Selected 2D classes. **(d)** Fourier Shell Correlation graph for final refinement. **(e)** Local resolution of final refined cryoEM map. **(f)** Architecture of the *M. brachiatum* UbI_3 filament, showing six UbI_3 dimers in alternating blue and orange. Bound Ca^{2+} ions are shown in gray on the cartoon diagram at right. **(g)** Closeup views of Ca^{2+} ions bound at sites 1 (intra-dimer), 3 (inter-dimer), and 4 (inter-dimer).